Phase Index Calculation for Anatomical Reentry Using Cross-correlation

Arthur S Bezerra, Sander Hendrickx, Robin Van den Abeele, Eike M Wülfers, Bjorn Verstraeten, Sebastiaan Lootens, Arstanbek Okenov, Timur Nezlobinsky, Nele Vandersickel

Department of Physics and Astronomy, Ghent University, Ghent, Belgium

Abstract

We previously showed that reentry in atrial tachycardia (AT) consistently occurs in pairs around two critical boundaries (CBs), which when connected by an ablation line consistently stops the AT. CBs can be identified by calculating the phase index (PI) using local activation times (LATs). However, LATs can be challenging to identify, especially in more complex arrhythmias. To overcome this limitation, we used a novel method using signal cross-correlation. We compared both methods (LAT versus signal) through 380 spherical simulations of anatomical reentry. 1610 evenly placed unipolar electrograms (EGMs) were generated for each simulation. After pre-processing, we derived (1) LATs, and (2) time delays through cross-correlation. PI was calculated as the sum of (1) LAT differences or (2) correlation-delays, divided by the cycle length. To test robustness, both methods were repeated after adding white Gaussian noise to the original EGMs, with decreasing signal-to-noise ratios (SNR = 10 dB, 5 dB, 0 dB). With no noise, both methods had 100% accuracy. As SNR decreased, the cross-correlation method showed consistently superior accuracy (LAT: 96.1%, 94.1%, and 77.4%, cross-correlation: 100%, 98.6%, and 83.5%). Our results validate the greater robustness of cross-correlation to identify ablation targets thought PI, while avoiding direct LAT annotation.

1. Introduction

Cardiac arrhythmias such as atrial tachycardia (AT) and atrial fibrillation (AF) are commonly treated using radiofrequency catheter ablation guided by an electroanatomical system. For AT, ablation is commonly guided using local activation time (LAT) mapping. This technique involves the use of intracardiac electrogram (EGM) signals to estimate the times at which the electrical wavefront passes each mapping point within the heart [1]. LAT maps are commonly used to aid electrophysiologists in identifying anatomical reentry circuits – self propagating activation waves that move around anatomical boundaries such as veins or valves.

Recently, we have theoretically and clinically shown the importance in AT of the paired loop paradigm (PLP), which states that reentries must always come in pairs of clockwise and counter-clockwise rotations [2–4]. However, these paired rotations have often been overlooked due to the existence of partial reentries – where a wave rotates around a boundary but collides with the next pulse before completing the rotation. Figure 1 illustrates the possible types of activity around a boundary – full reentry, partial reentry, and no reentry.

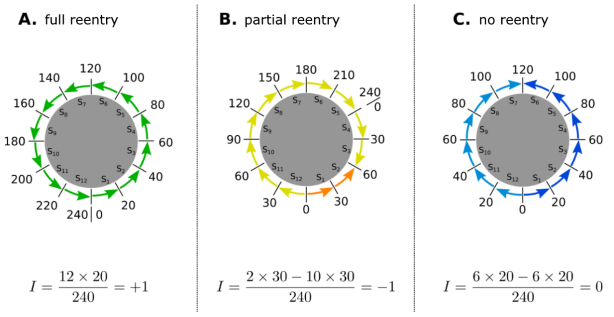

Figure 1. Example illustrating the three types of activity around a boundary. It shows the LATs around each boundary, and how differences in LAT can be used to calculate the phase index around each one, when normalized by the cycle length of 200 ms. CBs have index of +1 or -1, and non-CBs have index of 0.

Partial reentries are ablation targets as important as full reentries to terminate AT. If a partial reentry is not ablated along its paired full reentry, the partial reentry will become a new full reentry, creating a new pair and perpetuating the arrhythmia. We have previously described an LAT-based method to calculate the phase index (PI) which can identify critical boundaries (CBs) – anatomical boundaries where either a full reentry or a partial one are present [2–4]. However, the method suffers from a limitation: the dependence on LAT annotation.

In the case of low-voltage, high-noise, or fractionated signals, both unipolar and bipolar EGMs become less reliable measures of the LAT, as their morphology is significantly affected. Such cases are particularly common in AF

data, due to its turbulent and chaotic nature, but may even be found in AT cases, especially around scar tissue [5–7].

Therefore, the goal of this work is to propose an LAT-independent extension of our method, based on signal cross-correlation. As a proof-of-concept, we compared the new method to the already verified LAT-based results in 380 AT simulations, and then tested for robustness by introducing different noise levels.

2. Methods and materials

2.1. Dataset

We analyzed a simulated dataset consisting of 380 spherical surfaces with 20 mm radius, with non-conducting circular areas of varying sizes and distances between them, which represent the anatomical boundaries around which reentries can form (200 3-boundary cases, 180 4-boundary cases). The dataset was generated through OpenCarp [8], using the Ten Tusscher-Noble-Noble-Panfilov model [9] with the L-type calcium current reduced by 70% and the rapid delayed rectifier current increased by 70% in order to shorten the action potential for increased rotational stability. This cell model was subsequently pre-paced, using a pacing interval (S1-S1) of 250 ms for a duration of 5 seconds to reach a steady state [10]. For each simulation, 1610 evenly spaced unipolar EGMs were evaluated for a duration of 1.8 s, at a sampling frequency of 1 KHz.

The ground truth for each case – whether or not each boundary was a CB – was annotated by simulating the effects of creating an ablation line between each pair of boundaries for that case. On all simulations, only one pair of boundaires could terminate the reentry, as expected from the PLP, and those two were annotated as the CBs. Whether the CBs were full or partial reentries was not relevant for their detection or for ablation outcomes.

To evaluate the robustness of each method, they were evaluated in the original dataset, as well as after adding white Gaussian noise to the EGMs at signal-to-noise ratios (SNRs) of 10 dB, 5 dB, and 0 dB.

2.2. LAT-based PI

To identify each simulated case's CBs, we calculate the PI of all boundaries. For each boundary, EGM collection points that were up to 5 mm away from it were separated into N = 12 equal-sized sections, based on their angle relative to the center of the boundary. LATs were extracted from each EGM, and the average LAT for each section was obtained. The PI can then be calculated by calculating LAT-differences between each section and taking into account the cycle length (CL), as illustrated in Figure 1. The differences are then normalized by the CL to obtain a value of +1 or -1 depending on the direction of rotation. The following equation describes the PI computation:

$$PI = \frac{1}{CL} \sum_{i=0}^{N} (\overline{LAT_i} - \overline{LAT_j}) \; (mod \, CL) \qquad (1)$$

Where i indicates the placement of each section when ordered counter-clockwise, $j = i + 1 \; (mod \; N)$ is the next section in the counter-clockwise direction, and $\overline{LAT_i}$ is the mean LAT of section i.

2.3. Signal-based PI

In our new method, the same divison into sections around each boundary is done. Then, a 4-step pipeline is applied to obtain time-differences between EGM collection points of adjacent sections, as illustrated in figure 2.

First, a pre-processing pipeline common in the cardiac arrhythmia literature was used to smooth the EGMs: bandpass filtering in the band 40-250 Hz, followed by rectification and a lowpass filter with 20 Hz cutoff [11]. Signals were then mean-subtracted and normalized.

Second, all signals were sampled from a fixed time window with duration of $2\,CL$. This window replaces the need for the use of modular algebra applied in the LAT method.

Third, the cross-correlation was calculated between each pair of EGMs belonging to adjacent sections. For two real-valued discrete-time signals f and g, the discrete-time cross-correlation $(f \star g)$ is a function of the delay n, defined as:

$$(f \star g)[n] = \sum_{m=-\infty}^{\infty} f[m-n]g[m] \qquad (2)$$

The cross-correlation functions as a measure of morphological similarity between the signals, so when one signal is a time-shifted version of the other, a peak appears in the corresponding time-delay between them. For signals with periodic or quasi-periodic behavior, multiple correlation peaks may appear.

Finally, a range of acceptable physiological conduction velocity (CV) values between 0.2 mm/ms and 2 mm/ms was combined with the distance between each pair of points to obtain a range of acceptable time differences between each pair of points. Delays outside the physiological range were discarded, and if exactly one possible delay remained, that pair of points was used in the PI calculation.

With the time-delays between the different sections estimated, PI was then computed. The following equation describes this process, similar to the LAT-based method, but replacing the difference in $\overline{LATs}$ with mean correlation delays between sections.

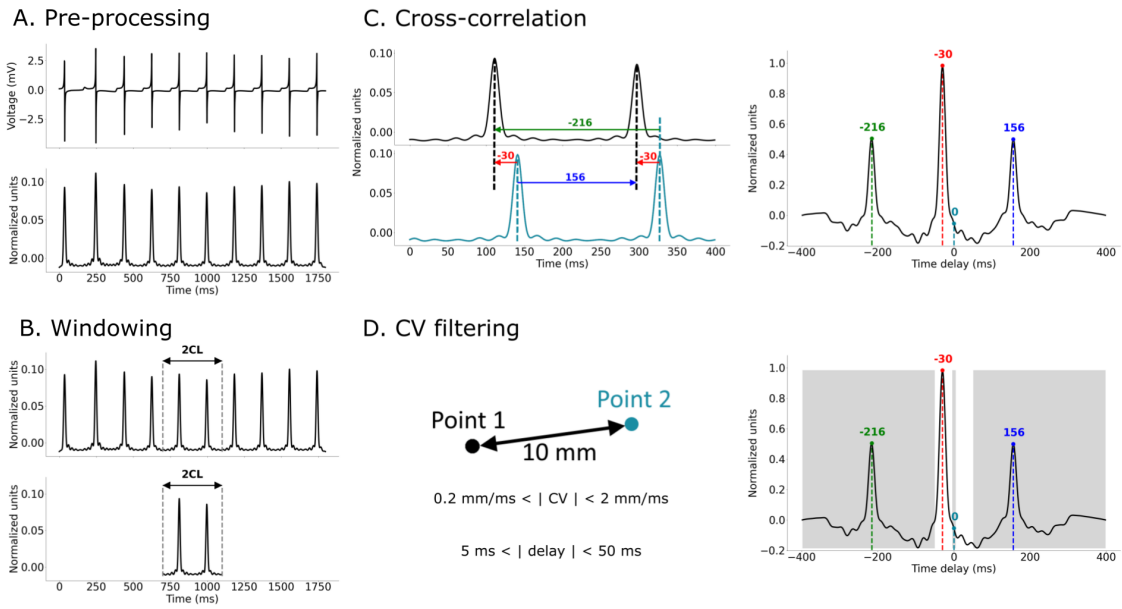

Figure 2. Diagram summarizing the steps taken to obtain time delay between EGMs. (A) An EGM is shown before (top) and after (bottom) pre-processing. Both signals become smoother and their activation peaks are highlighted. (B) The same EGM before (top) and after (bottom) applying a window at the center with duration of 2 CL. (C) A pair of signals (left) and the resulting cross-correlation between them (right). Peaks in the cross-correlation are candidates for the time difference between the signals. (D) From the distance between the points and the CV range, a time-delay range can be determined (left), and values outside that range are discarded, shown in gray (right).

$$PI = \frac{1}{CL} \sum_{i=0}^{N} \overline{\tau_{i,j}} \tag{3}$$

Where i and j represent the same as in equation (1), and $\overline{\tau_{ij}}$ is the mean correlation-delay between all EGMs in section i and all EGMs in section j.

2.4. Performance measurement

A boundary was considered correctly identified when the difference between its calculated PI and its ground truth (1 for CB, 0 otherwise) was less than .5. From this definition, accuracy in identifying boundaries was calculated for both methods at the different SNR levels.

3. Results

In the noiseless dataset, both methods achieved 100% accuracy. As SNR decreased, both methods had degraded performance, but the cross-correlation method had consistently superior performance to the LAT method. For the SNR values of 10 dB, 5 dB, and 0 dB, the LAT-based method had accuracy of 96.1%, 94.1%, and 77.4% respectively, while the cross-correlation method had accuracy of 100%, 98.6%, and 83.5% respectively. Figure 3 illustrates the evolution of performance with SNR for each method.

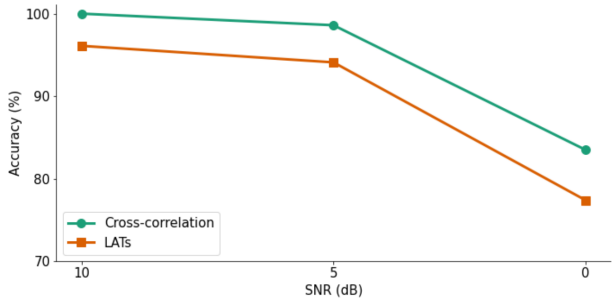

Figure 3. Accuracy as a function of SNR for the LAT and cross-correlation methods.

4. Discussion and Conclusion

We have introduced a new method for identification of CBs, based on the calculation of PI using the cross-correlation, rather than LATs. We have previously shown that PI is capable of identifying CBs consistently in clinical and simulated cases [2–4], but the method remained susceptible to the calculation of LATs. We have now solved this problem, with a method that displays comparable per-

formance in noiseless conditions, and greater robustness in the presence of noise.

Previous works have shown that cross-correlation can be more robust than direct LAT annotation when identifying time differences between signals, though not in the context of computing phases as done here [12, 13]. While several works in the literature have used phase calculation to identify functional reentry, it is typically not done with cross-correlation, but either from LATs, which is less robust, or through the Hilbert transform, which is more abstract. Additionally, to our knowledge, phase calculation is not commonly used to identify anatomical reentry [14, 15].

Finally, while the theoretical basis of the PLP has been known for years, it has not yet reached the clinics. This work aims to be another step towards bringing it to clinical use, potentially improving AT ablation procedures by avoiding AT recurrence and reducing ablation times and number of procedures.

Acknowledgments

This research was supported by VLIR/iBOF project "DIAMOND" (Grant 20-VLIR-iBOF-027), and a 'Starting Grant' from the European Research Council (ERC) under the European Union's Horizon 2020 research and innovation program (Grant No. 900008), awarded to Nele Vandersickel.

References

[1] El Haddad M, Houben R, Stroobandt R, Van Heuverswyn F, Tavernier R, Duytschaever M. Algorithmic detection of the beginning and end of bipolar electrograms: implications for novel methods to assess local activation time during atrial tachycardia. Biomedical Signal Processing and Control 2013;8(6):981–991.

[2] Vandersickel N, Hendrickx S, Van Den Abeele R, Wuelfers E, Bezerra A, Fuenmayor S, Duytschaever M, Knecht S, Haas A, Luik A. Unique topological classification of complex reentrant atrial tachycardias enables optimal ablation strategy. Europace 2023;25(Supplement_1):euad122–078.

[3] Vandersickel N, Hendrickx S, Van den Abeele R, Verstraeten B. Impact of topology on the number of loops during macro-re-entrant atrial tachycardia. European Heart Journal February 2024;45(18):1586–1588. ISSN 1522-9645.

[4] Duytschaever M, Abeele RVD, Carlier N, Bezerra A, Verstraeten B, Lootens S, Desplenter K, Okenov A, Nezlobinsky T, Shah D, Haas A, Luik A, Martens J, Haddad ME, Smet MD, Becker BD, François C, de Waroux JBLP, Tavernier R, Knecht S, Hendrickx S, Vandersickel N. Atrial topology for a unified understanding of typical and atypical flutter. Circulation Arrhythmia and Electrophysiology 2024;.

[5] Konings K, Kirchhof C, Smeets J, Wellens H, Penn OC, Allessie MA. High-density mapping of electrically induced atrial fibrillation in humans. Circulation 1994;89(4):1665–1680.

[6] van der Does LJME, de Groot NMS. Inhomogeneity and complexity in defining fractionated electrograms. Heart Rhythm 2017;.

[7] Fambuena-Santos C, Hernández-Romero I, Molero R, Atienza F, Climent AM, Guillem MS. Af driver detection in pulmonary vein area by electropcardiographic imaging: Relation with a favorable outcome of pulmonary vein isolation. Frontiers in Physiology 2023;14:1057700.

[8] Plank G, Loewe A, Neic A, Augustin C, Huang YL, Gsell MA, Elias Karabelas Mark Nothstein JS, Prassl AJ, Seemann G, Vigmond EJ. The openCARP simulation environment for cardiac electrophysiology 2021;.

[9] ten Tusscher KHWJ, Panfilov AV. Alternans and spiral breakup in a human ventricular tissue model. American Journal of Physiology Heart and Circulatory Physiology Sep 2006;291(3):H1088–H1100.

[10] ten Tusscher KH, Noble D, Noble PJ, Panfilov AV. A model for human ventricular tissue. Am J Physiol Heart Circ Physiol Apr 2004;286(4):H1573–1589.

[11] Botteron GW, Smith JM. Quantitative assessment of the spatial organization of atrial fibrillation in the intact human heart. Circulation 1996;.

[12] Shors SM, Sahakian AV, Sih HJ, Swiryn S. A method for determining high-resolution activation time delays in unipolar cardiac mapping. IEEE Transactions on Biomedical Engineering 1996;43(12):1192–1196.

[13] Cantwell CD, Roney CH, Ng FS, Siggers JH, Sherwin S, Peters NS. Techniques for automated local activation time annotation and conduction velocity estimation in cardiac mapping. Computers in Biology and Medicine 2015; 65:229–242.

[14] Valinoti M, Berto F, Alessandrini M, Mantovan R, Loewe A, Dössel O, Severi S, Corsi C. Phase analysis of endoatrial electrograms for 3d rotor detection in atrial fibrillation. In 2017 Computing in Cardiology (CinC). IEEE, 2017; 1–4.

[15] Arno L, Quan J, Nguyen N, Vanmarcke M, Tolkacheva EG, Dierckx H. Phase defect lines during cardiac arrhythmias: from theory to experiment. ArXiv Preprint 2021;.

Address for correspondence:

Arthur S Bezerra
Proeftuinstraat 80, Ghent 9000, Belgium
arthur.bezerra@ugent.be